Poly(4-methyl-1-pentene)-Supported Polyelectrolyte Multilayer Films: Preparation and Gas Permeability[1]

Juha-Matti Leväsalmi and Thomas J. McCarthy*

Polymer Science & Engineering Department, University of Massachusetts, Amherst, Massachusetts 01003

Received August 16, 1996; Revised Manuscript Received January 14, 1997[⊗]

ABSTRACT: Spontaneous sequential adsorption of poly(allylamine hydrochloride) and poly(sodium styrene sulfonate) (layer-by-layer deposition) onto surface-oxidized poly(4-methyl-1-pentene) film was studied with the objective of creating an asymmetric gas separation membrane consisting of a thin multilayer barrier layer on a more permeable polymer film. Poly(4-methyl-1-pentene) film was first surface-oxidized with chromic acid solution to introduce carboxylic acid functionality to the surface for depositing the first layer. By alternating the poly(allylamine hydrochloride) and poly(sodium styrene sulfonate) depositions, multilayered structures were prepared with the total number of layers up to 104. Gas permeabilities of composite membranes prepared by this layer-by-layer deposition technique were determined for hydrogen, oxygen, and nitrogen. The depressed gas permeabilities of the composite membranes are explained by dense and rigid packing of the polyelectrolytes in stratified layers. The multilayered poly(allylamine hydrochloride) and poly(sodium styrene sulfonate) structures were shown to be 18 000 times better barriers to nitrogen than poly(4-methyl-1-pentene). Alternating deposition of polyaniline and poly(sodium styrene sulfonate) into stratified multilayers on surface-oxidized poly(4-methyl-1-pentene), on the other hand, did not change the permeability properties of the film, suggesting a loose packing of molecules in the layers.

Introduction

Chemical and physical surface modifications can be used to significantly alter the gas permeability properties of a polymer film. We recently reported a study of the heterogeneous (gas−solid) chlorination of poly(4-methyl-1-pentene) as a surface-chemical approach for preparing asymmetric gas separation membranes.[2] Membranes of this type (asymmetric) have most often been prepared by phase inversion or by constructing composite structures. In the composite structure approach, dimensional constraint of molecules in ultrathin coatings may lead to improvements in gas barrier properties of a polymer film; however, the traditional methods of preparing ultrathin multilayered structures have numerous deficiencies. They may lead to intermixing of layers (solution casting and annealing techniques), have restrictions in the sample size (Langmuir−Blodgett), or require 100% reaction yields in order to maintain the functionality density at the surface (chemisorption).

Decher[3,4] and co-workers made use of earlier experimental[5,6] and theoretical work[7,8] on interactions between polyelectrolytes and charged surfaces and introduced "layer-by-layer deposition of polyelectrolytes" as a novel method for preparing ultrathin multilayers. Decher and others[9−17] have demonstrated the versatility and simplicity of this technique. The method is (normally) based on electrostatic attraction between anionic and cationic polymer species. An ultrathin layer is formed by dipping a substrate with a charged surface into a solution containing a polyelectrolyte of opposite charge. As a monolayer of the polyelectrolyte is deposited onto the substrate, the original surface charge is reversed and repulsive ionic forces prevent further deposition from taking place. The chain conformation of the deposited molecule, and thus also the layer thickness, are determined by the pH, ionic strength, and polyelectrolyte concentration of the dipping solution. Submerging the new surface in a solution of an oppositely charged polyelectrolyte causes another monolayer to deposit, and multilayers can be formed by alternating the dipping solutions.

We report here the use of poly(4-methyl-1-pentene) (PMP) film as a substrate for layer-by-layer polyelectrolyte deposition. We recently described the use of organic polymers as substrates for this process.[18] It was neccessary to chemically modify the PMP surface to introduce charge to support the initial layer deposition. Surface oxidation introduces carboxylic acid functionality that renders the surface negatively charged at sufficiently high pH. Polyelectrolyte multilayers self-assemble readily on the oxidized PMP surface. The gas permeabilities of the resulting asymmetric membranes are described.

Experimental Section

General Procedures. PMP film (50 μm Mitsui TPX) was extracted in refluxing dichloromethane for 1 h under nitrogen and dried at reduced pressure at room temperature to constant mass. Chromium(VI) oxide (Aldrich), sulfuric acid (Fisher), nitric acid (Fisher), 2-propanol (HPLC grade, Fisher), hydrochloric acid (1 N, Fisher), hydrogen peroxide (30%, Fisher), (4-aminobutyl)dimethylmethoxysilane (United Chemical Technologies), methanol (HPLC grade, Fisher), and toluene (HPLC grade, Fisher) were used as received. Poly(allylamine hydrochloride) (M_n 50000−65000, Aldrich) and poly(sodium styrene sulfonate) (M_n 70000, Aldrich) were used as received. Water was purified using a Millipore Milli-Q system that involves reverse osmosis followed by ion-exchange and filtration steps (resistivity better than 18.2 MΩ cm). Solution pH for layer-by-layer adsorption studies was adjusted with small amounts of either HCl or NaOH solution using a Fisher 825MP pH meter.

XPS spectra were obtained with a Perkin-Elmer Physical Electronics 5100 spectrometer using Mg Kα excitation (400 W, 15.0 kV). Spectra were recorded at a takeoff angle 75° (measured between the film surface plane and the entrance lens of the detector optics). Atomic composition data were determined using sensitivity factors obtained from samples of known composition: C_{1s}, 0.250; N_{1s} 0.420; S_{2p} 0.540; O_{1s}, 0.628; Cl_{2p}, 0.655. Attenuated total reflectance infrared (ATR IR)

[⊗] Abstract published in *Advance ACS Abstracts,* March 1, 1997.

S0024-9297(96)01245-4 CCC: $14.00

spectra were recorded using an IBM 38 FTIR at 4 cm^{-1} resolution with a 10 × 5 × 1 mm 45° Ge internal reflection element. Gravimetric measurements were made with a Sartorius 1612MP-1 analytical balance. Dynamic advancing (θ_A) and receding (θ_R) contact angles were measured with a Ramé-Hart telescopic goniometer and a Gilmont syringe with a flat-tipped 24-gauge needle as probe fluid was added (θ_A) or withdrawn (θ_R) from the drop. Phase interference microscopy was performed using a Zygo Maxim 3D Model 5700.

Surface Oxidation of Poly(4-methyl-1-pentene). Clean PMP films were surface-selectively oxidized by a method that was a modification of the polyethylene oxidation reported by Rasmussen et al.[19] Both sides of the film were reacted, while the CrO_3 concentration in 28 vol % H_2SO_4(aq), temperature, and reaction time were controlled. The films were further treated with 70% HNO_3(aq) at 50 °C for 30 min, washed with five cycles of alternating baths of water and 2-propanol, and stored under reduced pressure overnight before the first polyelectrolyte layer was deposited.

Surface Modification of Silicon Wafers. Silicon wafers were cleaned by reacting the surface for 15 min in 30 vol % H_2O_2 (30%) solution in concentrated sulfuric acid. Wafers were then washed with running water for 15 min, dried in a stream of air, and placed in a closed reaction vessel under clean room atmosphere. Wafers were washed under nitrogen in methanol (3×), 1:1 methanol/toluene mixture (3×), and toluene (3×) before reacting both surfaces of the samples in 1 vol % (4-aminobutyl)dimethylmethoxysilane solution in toluene for 16 h. After the coupling reaction, the samples were washed with the same series of solvents, but in reverse order. The amine-functionalized silicon wafers were used for layer-by-layer deposition experiments immediately or after being stored overnight at reduced pressure.

Layer-by-Layer Depositions. Poly(allylamine hydrochloride) (PAH) and poly(sodium styrene sulfonate) (PSS) deposition solutions were prepared by dissolving 0.250 g of PAH and 0.750 g of PSS in 250 mL of water and adjusting pH to the desired value. Fresh deposition solutions were made for each day of adsorption. The first layer was deposited onto surface-oxidized PMP film on the day following the oxidation. Between depositions the samples were washed twice in water and once in water that was adjusted to the pH of the following deposition solution. A maximum of 10 layers was deposited daily before drying the samples in a stream of nitrogen and then at reduced pressure at room temperature overnight.

Determination of Multilayer Thickness. Total layer thicknesses were determined by X-ray reflectivity for a series of PAH/PSS multilayers on amine-functionalized silicon wafers. The samples were kept at reduced pressure in the test chamber for 24 h prior to the X-ray reflectivity measurement (1.54 Å, Cu target) under vacuum to determine dry thickesses.

Gas Permeation Rate Measurements. Gas permeation studies were run one gas at a time with hydrogen, oxygen, and nitrogen at 40 °C with an upstream pressure of 6 atm and a downstream pressure of 0 atm. After reaching a steady-state flux of gas, a pressure increase of 0.50 mm in a known volume on the downstream side was timed. A home-built pressure/vacuum manifold[2] was built around a Millipore 25 mm membrane cartridge and a Celesco DP 31 differential pressure transducer.

Results and Discussion

Substrate Preparation. The goal of oxidizing the PMP film surface was to create a surface with carboxylic acid functionality that could render a high charge density at the surface at sufficiently high pH. Chromic acid oxidations of PMP film samples in 28 vol % sulfuric acid solutions (aqueous) were studied at various reactant concentration, reaction temperatures, and times to maximize the oxygen content of the film (as assessed by X-ray photoelectron spectroscopy, XPS) and minimize degadation (as assessed by gravimetric analysis). The extent of oxidation was shown to increase roughly linearly with oxidant concentration and reaction temperature. The oxygen:carbon ratios reached a maximum value of ∼0.18 within the first 2 min upon oxidation at 80 °C in a saturated CrO_3 solution, as shown in Figure 1. Longer reaction times led to no increases in the extent of oxidation, but increased mass losses as the reaction proceeded by chain degredation. The carbonyl stretching band in the ATR IR spectrum revealed that at least some of the oxygen atoms were incorporated as carbonyl-containing functionalities. Comparison of the pH dependence of the advancing water (buffered solutions) contact angle for unmodified and surface-oxidized PMP samples (Figure 2) confirms that a considerable fraction of the carbonyl groups present are carboxylic acids as the wetting behavior of the oxidized surface changes as a function of pH. The lower contact angles at higher pH values indicate the presence of CO_2H that ionize to CO_2^- groups. Comparison of phase interference micrographs of clean PMP and surface-oxidized PMP show that the degradative oxidation does not result in any changes in surface roughness detectable by this analytical technique.

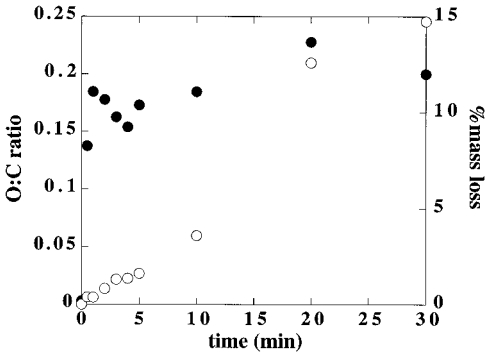

Figure 1. Kinetics of oxidation using 5 M CrO_3 solution in 28 vol % sulfuric acid at 80 °C: XPS oxygen:carbon ratio (●), percent mass loss (○).

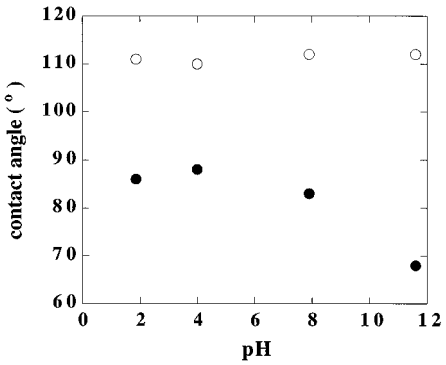

Figure 2. pH dependence of advancing water contact angle for unmodified (○) and surface-oxidized (●) PMP.

On the basis of the above analyses, the oxidized PMP surface contains a maximum of ∼1 ionizable carboxylic acid functionality per two PMP repeat units (assuming that all oxygen is in the form of carboxylic acids). As shown below, this reaction yields sufficiently high surface charge density and ionic interaction between the surface and the polyelectrolyte for the deposition of the first layer. The oxidized PMP surface is referred to as PMP−COOH below.

Layer-by-Layer Deposition of Polyelectrolytes onto PMP−COOH. The deposition kinetics and pH dependence were studied for PAH deposition onto the PMP−COOH surface, PSS deposition onto the PMP−COOH/PAH surface, and PAH deposition onto the PMP−COOH/PAH/PSS surface. Conditions were cho-

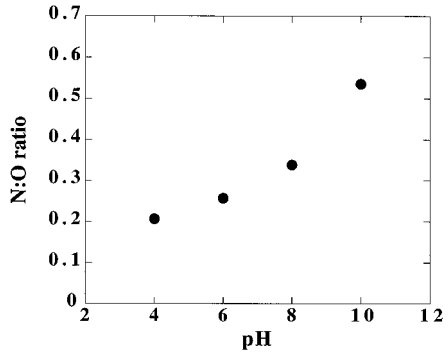

Figure 3. pH dependence of PAH self-assembly onto PMP−COOH. Nitrogen:oxygen atomic ratios after 60 min of deposition.

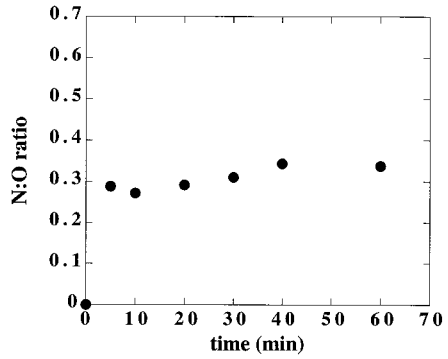

Figure 4. Kinetics of PAH self-assembly onto PMP−COOH at pH 8.

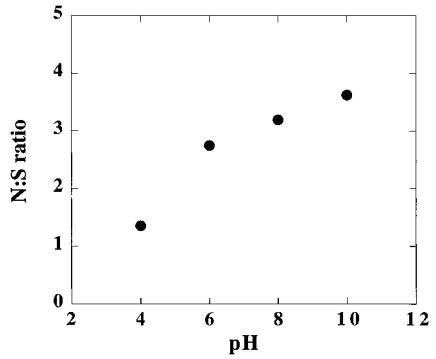

Figure 5. pH dependence of PSS self-assembly onto PMP−COOH/PAH. Nitrogen:sulfur atomic ratios after 10 min of deposition.

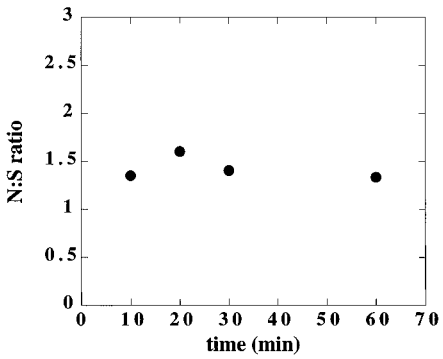

Figure 6. Kinetics of PSS self-assembly onto PMP−COOH/PAH at pH 4.

sen from these experiments for multilayer assembly. Multilayered structures were prepared by depositing additional PAH and PSS monolayers sequentially. The polyelectrolyte concentrations were chosen to be high enough that exhaustion of polyelectrolyte from the deposition solution was not a concern in the course of multiple depositions.

PAH Adsorption to PMP−COOH. PAH deposition kinetics were studied using 0.016 M dipping solutions at pH 4, 6, 8, and 10. At each pH level PAH was deposited onto the PMP−COOH surface for 5, 10, 20, 30, 40, and 60 min. The increase in nitrogen:oxygen ratio as a function of pH for a series of 60-min depositions are presented in Figure 3. The value of the atomic ratio, and thus the total amount of PAH deposited, increases linearly as the pH is increased from 4 to 8, due to deprotonation of carboxylic acid groups leading to enhanced ionic interaction between the surface and the adsorbing PAH molecule. The increase in nitrogen content that occurs between pH 8 and pH 10 can be attributed to the loss of charge−charge repulsions in deprotonated PAH (the pK_a of PAH is ∼10.6[20,21]). Depositions were also shown to incorporate very small amounts of chloride counterions onto the surface, but at a maximum level of one chloride per 10 nitrogen atoms, suggesting that most ammonium functionalities have carboxylate groups as counterions (this may not be the case: chlorine content is discussed below). On the basis of XPS analysis, the self-assembly was shown to reach a final state in less than 5 min at all the pH conditions studied. Deposition kinetics are presented in Figure 4 for the experiments at pH 8. Adsorption from 0.016 M PAH solution adjusted to pH 8 for 10 min was the condition chosen for further experiments.

PSS Adsorption to PMP−COOH/PAH. Deposition of PAH onto PMP−COOH creates a positively charged PMP−COOH/PAH surface. Deposition of PSS onto the PAH surface to build the second layer was studied using 0.015 M PSS solutions at pH 4, 6, 8, and 10 with deposition times ranging from 10 to 60 min. The sulfonate groups of PSS are ionized under all the pH conditions studied here; thus any pH dependence of the deposition is caused by changes in the ionic state of the PAH surface. The deposition of PSS onto the PMP−COOH/PAH surface exhibits the pH dependence shown in Figure 5. As the deposition solution becomes increasingly acidic, the ionic interactions are strengthened, leading to deposition of a self-assembled layer of PSS. This is seen in a decrease of the N:S atomic ratio as pH is lowered. The adsorption of PSS to PMP−COOH/PAH is also rapid; the kinetics for deposition at pH 4 (Figure 6) indicate that 10 min is sufficient time for the second layer to assemble. Similar to the formation of the first layer, the atomic compositions for the samples are practically identical, regardless of the deposition time. Conditions chosen for further experiments were 10 min from 0.015 M PSS solution adjusted to pH 4.

PAH Adsorption to PMP−COOH/PAH/PSS. The third deposition type in this system is the deposition of PAH onto a sulfonate surface. The sulfonate substrate was prepared as described above by depositing PSS onto PMP−COOH/PAH. Deposition of the third layer was studied changing the deposition times from 10 to 60 min in 0.016 M PAH solutions adjusted to pH values 4, 6, 8, and 10. Like the first two layer adsorptions, the third layer adsorbs rapidly, reaching a final composition (N:S ratio) in less than 10 min. The composition is essentially independent of pH from 4 to 8, but nitrogen content increases sharply at pH 10 for the reason described above. The conditions chosen for adsorption were the same as those used for the first layer: 10 min from 0.016 M PAH solution adjusted to pH 8.

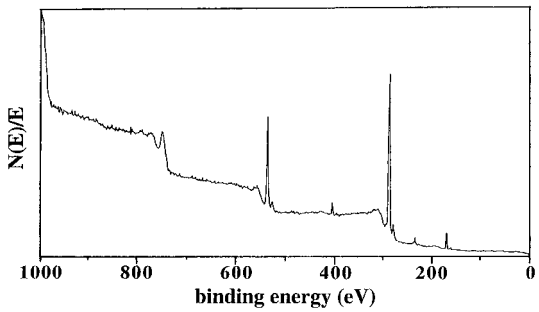

Figure 7. XPS survey spectrum of a PMP−COOH/PAH/PSS multilayer sample with 102 layers.

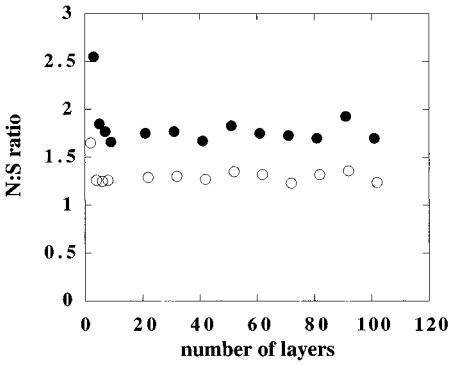

Figure 8. Nitrogen:sulfur atomic ratio data as a function of number of layers for a series of PMP−COOH/PAH/PSS samples: PAH top layer (●), PSS top layer (○).

Multilayer Depositions. PAH and PSS were layer-by-layer deposited onto PMP−COOH to build up multilayered composites using the conditions optimized for the first three layers. Between depositions the samples were rinsed sequentially in water baths; the last rinsing solution was adjusted to the pH of the subsequent deposition solution. The pH-adjusted rinse was used to minimize any solution transfer that could change the pH of the deposition solution.

A representative XPS survey spectrum of a PMP−COOH/PAH/PSS multilayer assembly (102 polyelectrolyte layers) is shown in Figure 7; the features of interest are present in this spectrum. The S_{2p} (164 eV), S_{2s} (230 eV), C_{1s} (285 eV), N_{1s} (398 eV), and O_{1s} (532 eV) photoelectron lines are apparent, and their relative intensities depend on the location and thickness of PAH and PSS layers within the XPS sampling region. If the deposited layers are well-defined (stratified), and there is not extensive mixing between the layers, data from surface-sensitive analytical techniques should strongly depend on which polyelectrolyte, PAH or PSS, was used in the last deposition step. The three components in the multilayered structures are "labeled" in their atomic composition: in the case of building stratified layers, one creates regions that are rich in oxygen (PMP−COOH), nitrogen (PAH), and sulfur (PSS).

The nitrogen:sulfur ratio (calculated from XPS atomic composition data) as a function of number of layers is presented in Figure 8. The scatter in the data is due primarily to the fact that separate samples were used for analysis of multilayers of each thickness (number of layers). Samples were not used after analysis as substrates for further depositions. For samples in which PAH was used in the last deposition step (odd number of layers), the N:S ratio has a value of ∼1.75. For samples containing PSS as the outermost layer, the N:S ratio is ∼1.25. This odd−even trend in alternating values for the N:S atomic ratio persists to high layer number (104 layers was the greatest number studied), where addition of one more PSS or PAH layer does not affect the overall composition significantly. This implies a layered structure which is consistently stratified. Considering the thickness of the layers (see below), there is certainly interpenetration of the layers at the dimension scale of the functional groups to ensure efficient packing of the molecules at the layer interfaces. We emphasize that the XPS analyses are carried out on dry films under high vacuum and the stratification observed under these conditions may not accurately reflect the structure of the hydrated layers during assembly.

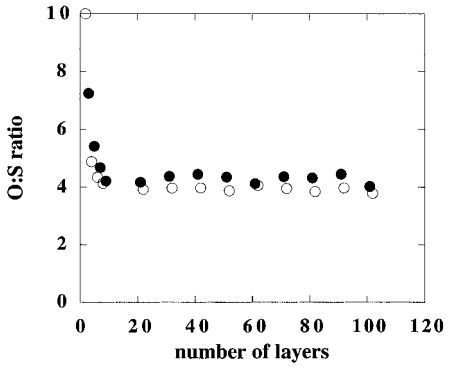

Figure 9. Oxygen:sulfur atomic ratio data as a function of number of layers for a series of PMP−COOH/PAH/PSS samples: PAH top layer (●), PSS top layer (○).

The N:S ratio of ∼1.5 for the multilayer structures indicates the stoichiometry of the assembly process: there are about three ammonium ions per two sulfonate ions in the multilayer assemblies. Chloride should be present as the counterion for the excess ammonium ion in all samples, but chlorine is observed by XPS to be present in only trace amounts and in many samples it is not observed at all. Our only explanation for the absence of chloride is that we analyze for it (by XPS) on dry films at very low pressures, and under these conditions HCl is lost to render free amines.

The oxygen:sulfur ratio as a function of number of layers is presented in Figure 9. For samples with only a few layers, the XPS sampling region includes the oxygen-rich PE−COOH substrate resulting in high O:S values. After ∼8 depositions, the value of the atomic ratio reaches an almost constant level of ∼4 indicating that a multilayer assembly of ∼8 layers has the thickness of the XPS sampling depth. The fact that sulfonate groups (the only component containing oxygen and sulfur that is detected by XPS at sufficient multilayer thickness) contain three oxygen and one sulfur and that the deposition of PAH onto a PSS surface causes the oxygen content to increase is most likely an indication of the presence of water molecules that are strongly bound to the structure (in the PAH layer in particular).

If the layers are stratified as indicated by the XPS analysis, contact angles of the multilayer surface should be sensitive to the wetting properties of the polyelectrolyte used in the last deposition step. The cosine of the advancing contact angle measured using water as the probe fluid is plotted versus the number of layers for multilayer films in Figure 10. The pronounced odd−even trend indicates that the surface energy of the multilayered samples depends greatly on which polyelectrolyte was used in the last deposition. Samples with PAH as the last deposited polyelectrolyte gave advancing contact angles of ∼83°, and deposition of PSS onto those surface lowers the angles to ∼50°, indicating

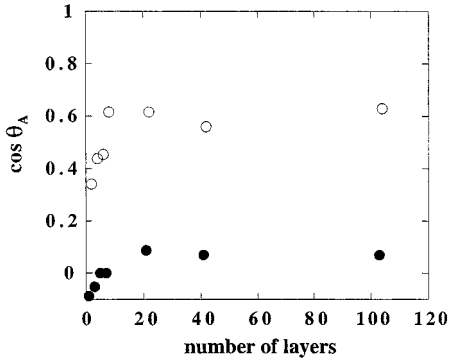

Figure 10. Cosine of the advancing contact angle with water as the probe fluid for a series of PMP−COOH/PAH/PSS samples: PAH top layer (●), PSS top layer (○).

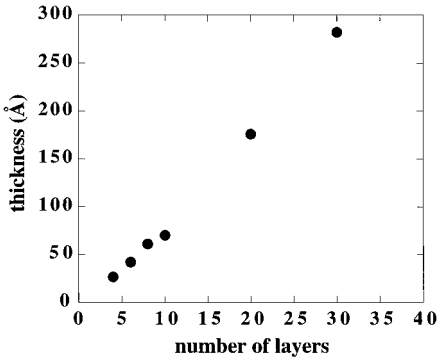

Figure 11. Thickness (X-ray reflectivity) of PAH/PSS multilayers on amine-functionalized silicon wafers.

that the polyelectrolytes form stratified layers with characteristic wetting properties.

Layer Thickness Determinations. Contact angle and XPS studies indicate that the layered structures are highly organized and stratified. In order to determine the average thickness of a layer, alternating monolayers of PAH and PSS were self-assembled onto amine-functionalized silicon wafers for X-ray reflectivity and XPS studies. The same polyelectrolyte deposition conditions were used. Samples were prepared with a total number of 2, 4, 6, 8, 10, 20, and 30 layers.

The silane coupling agent layer ($-SiMe_2CH_2CH_2CH_2-NH_2$) alone was too thin to be analyzed by the technique, and the reflectivity data for the sample with two layers could not be fitted to any electron density model, indicating a nonuniform coating on the wafer. Figure 11 shows that the total thickness of a multilayer assembly (including the coupling layer) increases almost linearly with the number of layers. For example the difference in thickness of samples with 20 and 30 layers equals that of samples with 10 and 20 layers. The thickness of a layer depends on its location in the multilayer structure: after about 10 depositions a consistent thickness of 10.6 Å is reached; the first 10 layers average 6.5 Å in thickness.

After the X-ray reflectivity measurements, the same samples were analyzed by XPS. The silicon:carbon ratios from XPS analysis are plotted as a function of number of layers in Figure 12. The silicon signal from the substrate is almost completely attenuated after ∼8 layers have been deposited. This observation is consistent with the disappearance of the oxygen signal from the PMP−COOH substrate (Figure 9), and this consistency indicates that the layers on the two substrates have similar thicknesses.

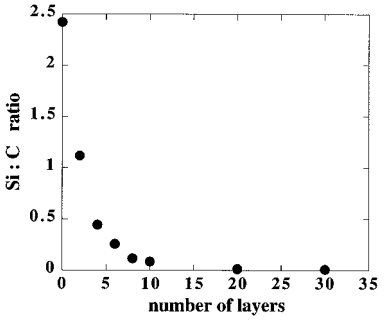

Figure 12. Silicon:carbon atomic ratios from XPS analysis for a series of multilayers on amine-functionalized silicon wafers.

Table 1. Gas Permeability of PMP−COOH/PAH/PSS Multilayer Membranes

sample	$P(N_2)^a$	$P(O_2)^a$	$P(H_2)^a$
PMP	1.3	5.4	22.0
PMP−COOH	1.3	4.1	17.5
PMP−COOH/PAH/PSS			
10 layers	0.95	4.2	16.8
20 layers	0.35	2.1	16.4
50 layers	0.13	1.0	13.3
100 layers	0.13	0.97	13.3
200 layers	0.08	1.2	9.7

^{a} 10^{-9} cm^3 (STP) cm/cm^2 s cm(Hg).

Table 2. Gas Selectivity of PMP−COOH/PAH/PSS Multilayer Membrane with 200 Layers

sample	O_2/N_2	H_2/N_2	H_2/O_2
PMP	4.2	16.9	4.1
PMP−COOH/PAH/PSS	15	121	8.1

Gas Permeability Measurements. Gas permeabilities of unmodified PMP, PMP−COOH, and a series of PMP−COOH-supported multilayer assemblies were determined to nitrogen, oxygen and hydrogen (Table 1). The number of layers indicated in Table 1 is the sum of the number of layers on both sides of the film, thus a 10-layer sample was prepared by five deposition cycles. Surface oxidation does not affect the gas permeability of PMP within experimental variation; however, deposition of PAH/PSS multilayers significantly lowers the permeability, even for the case of 10 layers.

Multilayer thickness determinations suggested that ∼10 deposition cycles are needed to create effectively packed layers of uniform thickness. A comparison of the effectiveness of five layers (a total of 10 layers on the membrane) and 10 layers (total of 20 layers) to reduce the flux of gas through the membrane supports this picture of packing efficiency as the diffusing gas molecules act as nanoprobes, relating the macroscopic permeability properties to differences in packing at the molecular level. Considering the relative thicknesses of the multilayered structures and the PMP substrate, we can calculate the barrier properties of the multilayered structure. For nitrogen, the multilayered structure is a better barrier than PMP by a factor of ∼18000. The multilayer membranes exhibit improved gas selectivities compared to those of PMP. Selectivities calculated from single gas experiments are reported for the composite membrane with 200 layers in Table 2.

The changes in gas permeability indicate that the polyelectrolytes are packed in the multilayer assemblies in a very dense and rigid manner. The multilayer assemblies can be regarded as assemblies of monolayers with the majority of repeat units of the polyelectrolytes ionically cross-linked to the monolayer below or above

it. The intersegmental distance in the defect-free layers must be comparable to the diameter of the gas molecules studied as considerably larger gaps between chain segments, or defects on a macroscopic scale would not give the observed significant reductions in gas permeation rates.

Conclusions

Self-assembly of polyelectrolytes into multilayers supported on PMP leads to well-defined structures that can be controlled at the molecular scale. Under suitable conditions, the technique enables the control of thickness of a coating with ~10 Å increments. For systems of high charge densities and strong ionic interactions, self-assembly results in close packing of polymer chains that are apparently immobilized by ionic cross-links between charged functionalities in repeat units. We propose that high restrictions in segmental motion within the layers leads to interesting macroscopic properties, as was shown for gas permeability in this work.

We chose PSS and PAH as polyelectrolytes because this system has been most widely studied. We have also studied polyaniline (pH 4, 90:10 (vol:vol) water/dimethylacetamide) and PSS layer-by-layer depositions onto the PMP−COOH surface, and XPS and contact angle analyses reveal that stratified multilayers similar to the PAH/PSS system form. The gas permeability properties of the composite membranes, however, were unchanged from those of PMP (up to 50 layers). This is likely due to lower ionic cross-link density that allows chain segments to accommodate gas permeation through the structure.

Acknowledgment. We thank Xiaoqun Zou and Scott Barton for the X-ray reflectivity measurements. Financial support from the Office of Naval Research, the University of Massachusetts CUMIRP program and Aerovox is acknowledged. J.-M.L. thanks the Neste Corporation Foundation for fellowship support.

References and Notes

(1) A preliminary account of this work has been presented: Leväsalmi, J.-M.; McCarthy, T. J. *Polym. Prepr. (Am. Chem. Soc. Div. Polym. Chem.)* **1996**, *37* (1), 457.
(2) Leväsalmi, J.-M.; McCarthy, T. J. *Macromolecules* **1995**, *28*, 1733.
(3) Decher, G.; Hong, J. D.; Schmitt, J. *Thin Solid Films* **1992**, *210/211*, 831.
(4) Lvov, Y.; Decher, G.; Mohwald, H. *Langmuir* **1993**, *9*, 481.
(5) Cosgrove, T.; Obey, T. M.; Vincent, B. J. *J. Colloid Interface Sci.* **1986**, *111*, 409.
(6) Blaakmeer, J.; Böhmer, M. R.; Cohen Stuart, M. S.; Fleer, G. J. *Macromolecules* **1990**, *23*, 2301.
(7) Evers, O. A.; Fleer, G. J.; Scheutjens, H. M.; Lyklema, J. *J. Colloid Interface Sci.* **1986**, *111*, 446.
(8) Van der Schee, H. A.; Lyklema, J. *J. Phys. Chem.* **1984**, *88*, 6661.
(9) Keller, S. W.; Kim, H. N.; Mallouk, T. E. *J. Am. Chem. Soc.* **1993**, *115*, 11855.
(10) Bell, C. M.; Arendt, M. F.; Gomez, L.; Schmehl, R. H.; Mallouk, T. E. *J. Am. Chem. Soc.* **1994**, *116*, 8374.
(11) Ferreira, M.; Rubner, M. F. *Macromolecules* **1995**, *28*, 7107.
(12) Fou, A. C.; Rubner, M. F. *Macromolecules* **1995**, *28*, 7115.
(13) Cheung, J. H.; Fou, A. C.; Rubner, M. F. *Thin Solid Films* **1994**, *244*, 985.
(14) Kleinfeld, E. R.; Ferguson, G. S. *Science* **1994**, *265*, 370.
(15) Mao, G.; Tsao, Y.; Tirrell, M.; Davis, H. T. *Langmuir* **1993**, *9*, 3461.
(16) Hammond, P. T.; Whitesides, G. M. *Macromolecules* **1995**, *28*, 7569.
(17) Decher, G.; Lvov, Y.; Scmitt, J. *Thin Solid Films* **1994**, *244*, 772.
(18) Chen, W.; McCarthy, T. J. *Macromolecules* **1997**, *30*, 78.
(19) Rasmussen, J. R.; Stedronsky, E. R.; Whitesides, G. M. *J. Am. Chem. Soc.* **1977**, *99*, 4736.
(20) Arnett, E. M. *Prog. Phys. Org. Chem.* **1963**, *1*, 223.
(21) Brown, H. C.; McDaniel, D. H.; Hflinger, O. In *Determination of Organic Structures by Physical Methods*; Braude, E. A., Nachod, F. C., Eds.; Academic Press: New York, 1955; p 567.

MA961245S